ELSEVIER

Journal of Alloys and Compounds 446–447 (2007) 101–105

Journal of ALLOYS AND COMPOUNDS

www.elsevier.com/locate/jallcom

Structure and hydrogenation properties of the ternary alloys $Ca_{2-x}Mg_xSi$ ($0 \leq x \leq 1$)

Hui Wu [a,b,*], Wei Zhou [a,c], Terrence J. Udovic [a], John J. Rush [a,b]

[a] *NIST Center for Neutron Research, National Institute of Standards and Technology, 100 Bureau Dr., MS 8562, Gaithersburg, MD 20899-8562, USA*

[b] *Department of Materials Science and Engineering, University of Maryland, College Park, MD 20742-2115, USA*

[c] *Department of Materials Science and Engineering, University of Pennsylvania, 3231 Walnut St., Philadelphia, PA 19104-6272, USA*

Received 25 September 2006; received in revised form 3 January 2007; accepted 4 January 2007
Available online 12 January 2007

Abstract

Partially Mg-substituted Ca_2Si alloys ($Ca_{2-x}Mg_xSi$, $0 \leq x \leq 1$) were synthesized via high-temperature evacuation of $CaH_2/MgH_2/Si$ ball-milled mixtures. Neutron diffraction refinements showed that $Ca_{2-x}Mg_xSi$ ($0 < x < 1$) samples are not single-phase solid-solutions, but rather $(1-x)Ca_2Si + xCaMgSi$ mixed phases. Hydrogen absorption measurements indicated that, although pure Ca_2Si ($x = 0$) is readily hydridable and forms an unusual amorphous-hydride phase, pure CaMgSi ($x = 1$) does not noticeably absorb hydrogen up to 7 MPa H_2 and 473–573 K. Thus, hydrogen absorption behaviors of the intermediate compositions ($0 < x < 1$) are dominated by the Ca_2Si component, as evidenced by the isotherm measurements and neutron vibrational spectra.

Keywords: Hydrogen storage; Calcium magnesium silicide; Neutron diffraction; Neutron vibrational spectroscopy; Isotherm

1. Introduction

To improve the hydrogen-cycling properties of light-metal elements, recent attention has turned to the use of destabilizing additives such as Si [1–2]. Alloy combinations such as Ca–Si and Mg–Si have been among the growing number of destabilized hydrogen-storage candidates currently under investigation. Recent studies of the preparation and storage properties of CaSi and Ca_2Si alloys by neutron methods and other techniques have revealed the structure and bonding of hydride phases created under different synthesis conditions (pressure, temperature, stoichiometry, etc.) [3–6]. The more Ca-rich Ca_2Si alloy has the potential for higher hydrogen uptake (i.e., 3.59 wt.% max. for full hydriding of Ca_2Si to $2CaH_2 + Si$) compared to CaSi (2.87 wt.% max.). Much effort has also been expended on Mg_2Si [1], which has hydrogen wt.% advantages over Ca_2Si, and where it was hoped that a destabilization cycle involving Mg_2Si hydrogenation to $2MgH_2 + Si$ would readily occur. However, the kinetics have been found to be too slow for direct rehydrogenation at reasonably low temperatures. It is not clear at present why this is the case. Nonetheless, it would be informative to understand how modifying Ca_2Si by partial Mg substitution might ultimately affect hydrogenation properties. Substituting the lighter Mg atom for Ca would potentially increase the maximum hydrogen wt.% compared to pure Ca_2Si, but it is not yet clear how the absorption/desorption cycling properties would be impacted.

Although Ca and Mg are both alkaline-earth metals, they form different hydride and silicide structures. MgH_2 possesses $P4_2/mnm$ symmetry [7], whereas CaH_2 possesses *Pnma* symmetry [8–9]. Mg_2Si forms a cubic antifluorite structure [10], whereas Ca_2Si crystallizes in an orthorhombic anti-$PbCl_2$ or Co_2Si-type structure [11]. A previous study of a 1:1 Ca_2Si–Mg_2Si binary mixture indicated a single-phase solid-solution CaMgSi can be formed, crystallizing in a Co_2Si-type structure like pure Ca_2Si [12]. Other single-phase compositions have yet to be reported for this binary system. In this paper, we explore the structure and hydrogen-absorption properties of partially Mg-substituted Ca_2Si ternary alloys, $Ca_{2-x}Mg_xSi$, within the composition range $0 \leq x \leq 1$.

* Corresponding author. Tel.: +1 301 975 2387; fax: +1 301 921 9847.
E-mail address: huiwu@nist.gov (H. Wu).

0925-8388/$ – see front matter © 2007 Elsevier B.V. All rights reserved.
doi:10.1016/j.jallcom.2007.01.018

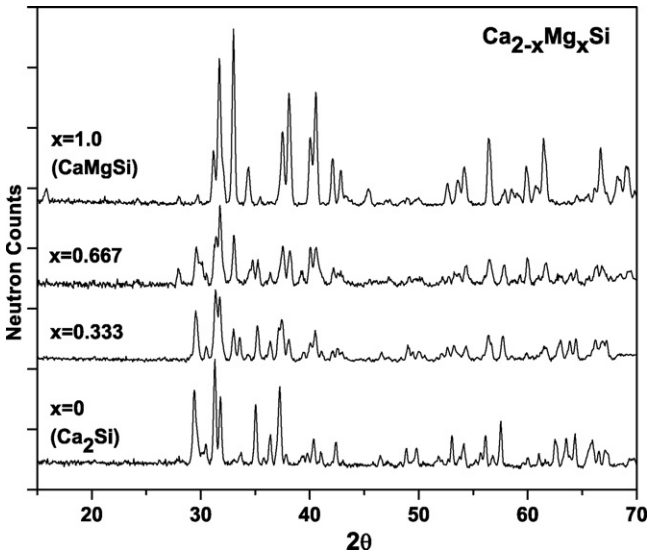

Fig. 1. Neutron powder diffraction patterns between 15° and 70° 2θ at 295 K for $Ca_{2-x}Mg_xSi$ ($x = 0$, 0.333, 0.667, and 1).

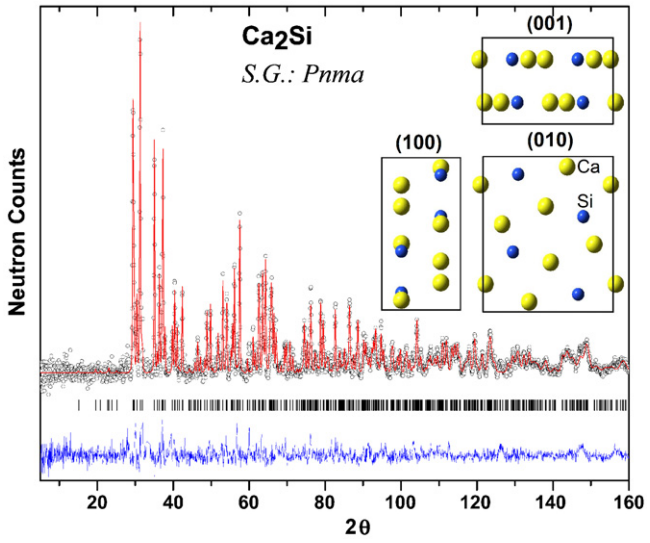

Fig. 2. Experimental (circles), calculated (line), and difference (line below observed and calculated patterns) NPD profiles at 295 K for Ca_2Si. The refined crystal structure in the [1 0 0], [0 1 0] and [0 0 1] projections is presented as insets. Large light and small dark spheres are Ca and Si, respectively.

2. Experimental

Four $Ca_{2-x}Mg_xSi$ powder samples (with $x = 0$, 0.333, 0.667, and 1) were synthesized via evacuation of ball-milled (400 rpm for 30 min), CaH_2 (Aldrich [13], 99.9%), plus MgH_2 (Alfa Aesar 98%) and Si (Alfa Aesar 99.999%) mixtures in the appropriate Ca:Mg:Si stoichiometric ratios. For $x = 0$, the evacuation occurred at 873 K for 10 h. For $x > 0$, the evacuation temperature was decreased to 723–773 K. Sample handling was performed in a He-filled glovebox to avoid oxidation reactions. All measurements were carried out at the NIST Center for Neutron Research. The isotherm measurements were performed using a Sieverts-type volumetric system. The neutron powder diffraction (NPD) data were collected using the BT-1 high-resolution powder diffractometer [14] with the Cu(311) monochromator at a wavelength of 1.5403(2) Å and an in-pile collimation of 15 min of arc. Data were collected over the 2θ range of 3–168°. Rietveld structural refinements were done using the GSAS package [15]. The neutron vibrational spectra were measured using the BT-4 Filter-Analyzer Neutron Spectrometer [16] with the Cu(2 2 0) monochromator under conditions that provided full-width-at-half-maximum (FWHM) energy resolutions of 2–4.5% of the incident energy over the range probed. The determination of hydrogen contents was accomplished via neutron prompt-gamma activation analysis (PGAA) using the NG-7 instrument.

3. Results and discussion

Since, the crystal structure of Ca_2Si contains equal proportions of two distinctive cation sites, it is not surprising that a ternary CaMgSi phase with segregated cations also possesses the same orthorhombic Co_2Si-type structure [12]. Previous studies of the analogous $Ca_{2-x}Mg_xSn$ system [17] indicated that a single-phase, solid-solution region only exists for $x \leq 1$, crystallizing in a Co_2Si-type structure. We have extended our studies to the $Ca_{2-x}Mg_xSi$ system, so as to test the hydrogen absorption properties of the possible mixed-light-metal solid solutions up to the highest possible Mg concentration (i.e., with the highest potential hydrogen capacity).

Fig. 1 shows the lower angle portion of the NPD patterns for all four $Ca_{2-x}Mg_xSi$ samples synthesized. In contrast to their Sn analogues, a single-phase solid-solution is found to be formed only at $x = 0$ (Ca_2Si) and $x = 1$ (CaMgSi). Fig. 2 displays the complete NPD pattern for Ca_2Si, which contains only lines of a Co_2Si-type orthorhombic structure (*Pnma*) with refined lattice parameters $a = 7.6910(3)$ Å, $b = 4.8174(1)$ Å, $c = 9.0477(3)$ Å, in good agreement with values reported in Ref. [11]. Fig. 3 shows the complete NPD pattern for CaMgSi, which exhibits a *Pnma* orthorhombic, cation-ordered structure with lattice parameters $a = 7.4934(2)$ Å, $b = 4.4384(1)$ Å and $c = 8.3345(4)$ Å, in good agreement with values reported in Ref. [12]. The CaMgSi sample also includes a small amount of Mg_2Si and Ca_2Si, probably

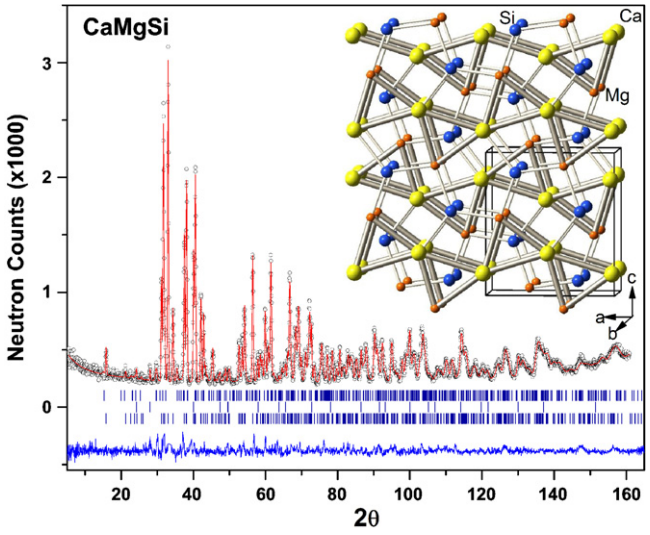

Fig. 3. Experimental (circles), calculated (line), and difference (line below observed and calculated patterns) NPD profiles at 295 K for CaMgSi. Vertical bars indicate the calculated positions of Bragg peaks for CaMgSi, Mg_2Si and Ca_2Si (from bottom to top). The refined crystal structure for CaMgSi is illustrated as an inset. Large light and small darker spheres represent Ca and Mg, respectively; medium dark gray spheres are Si. Shaded and horizontal trigonal prisms emphasize the chains of trigonal prismatic columns for cations. Light thin bonds are shown between Si and the cations (2 Mg and 1 Ca) that interconnect the chains.

Table 1
Crystallographic data refined from NPD patterns for $Ca_{2-x}Mg_xSi$

Space group (*Pnma* No. 65)			Ca_2Si			CaMgSi
			$x=0$	$x=0.333$	$x=0.667$	$x=1$
T (K)			295	295	295	295
F_{Ca_2Si} (wt.%)			100	72.08(4)	36.96(5)	7.23(3)
a (Å)			7.6910(3)	7.6835(4)	7.6829(9)	7.670(8)
b (Å)			4.8174(1)	4.7912(3)	4.7940(5)	4.814(2)
c (Å)			9.0477(3)	8.9994(6)	8.998(1)	8.975(3)
V (Å^3)			335.226(28)	331.306(39)	331.413(60)	331.3(3)
F_{CaMgSi} (wt.%)			–	28.92(4)	60.58(4)	90.32(6)
a (Å)			–	7.4944(9)	7.4936(8)	7.4934(2)
b (Å)			–	4.4398(4)	4.4387(4)	4.4384(1)
c (Å)			–	8.3363(9)	8.3356(5)	8.3345(4)
V (Å^3)			–	277.386(54)	277.257(52)	277.201(24)
F_{Mg_2Si} (wt.%)			–	–	2.46(6)	2.45(1)
a_{Mg2Si}			–	–	6.3537(3)	6.3564(2)
Ca1	4*c*	x	0.5207(4)	–	–	0.5195(2)
		z	0.6759(3)	–	–	0.6790(2)
		U_{iso}	1.99(6)	–	–	1.22(5)
Ca2/Mg1	4*c*	x	0.6545(4)	–	–	0.6431(2)
		z	0.0730(3)	–	–	0.0625(2)
		U_{iso}	1.49(6)	–	–	1.27(5)
Si	4*c*	x	0.2552(5)	–	–	0.2701(2)
		z	0.1072(3)	–	–	0.1148(3)
		U_{iso}	1.06(6)	–	–	1.10(5)
R_{wp}			0.0580	0.0594	0.0478	0.0600
R_p			0.0460	0.0461	0.0379	0.0437
χ^2			1.484	1.171	1.153	1.958

due to local inhomogeneity. The samples with $x=0.333$ and $x=0.667$ are mainly comprised of Ca_2Si/CaMgSi mixtures in the ratios of ≈2:1 and ≈1:2, respectively. A small amount of Mg_2Si was also detected for the $x=0.667$ composition. All refined crystallographic data for $Ca_{2-x}Mg_xSi$ ($x=0$, 0.333, 0.667 and 1) are summarized in Table 1.

Fig. 4 displays the hydrogen absorption isotherms at 473 K measured for different $Ca_{2-x}Mg_xSi$ compositions. It should be noted that plotting the isotherms for each sample with pressure on a logarithmic scale (Fig. 4b) illustrates the general lack of an obvious pressure plateau. In contrast to the difficulty of hydriding Mg_2Si [1], isotherm measurements on Ca_2Si show quite rapid hydrogen absorption (typically taking only several minutes for completion), even under relatively low H_2 pressure (<0.1 MPa), and a maximum hydrogen capacity of ≈2.1 wt.% is achieved at moderate pressures (<3 MPa). This absorption behavior makes Ca_2Si an intriguing system for hydrogen storage. For CaMgSi, the hydrogen uptake is essentially completely inhibited for conditions up to 7 MPa H_2 and 473–573K. It is notable from Fig. 4 that the maximum hydrogen uptake for the different samples systematically decreases in a linear fashion with increasing Mg concentration. Moreover, the ratio of maximum hydrogen uptakes for $Ca_{2-x}Mg_xSi$ and Ca_2Si samples, respectively (i.e., 2/3 for $x=0.333$, 1/3 for $x=0.667$) is roughly equal to the phase fraction of Ca_2Si in the corresponding compositions. (N.B.: $Ca_{2-x}Mg_xSi$ can be also viewed as a $(1-x)Ca_2Si + xCaMgSi$ mixture.) Thus for the Ca_2Si/CaMgSi mixed-phase samples, this is evidence that only the Ca_2Si component (and unfortunately not the CaMgSi component) is readily hydrided under the temperatures and pressures of this study.

Fig. 5 illustrates the neutron vibrational spectra for the hydrides of Ca_2Si, $Ca_{1.667}Mg_{0.333}Si$ and $Ca_{1.333}Mg_{0.667}Si$ formed at 7 MPa and 473 K. PGAA measurements indicated corresponding compositions of $Ca_2SiH_{2.41}$, $Ca_{1.667}Mg_{0.333}SiH_{1.41}$, and $Ca_{1.333}Mg_{0.667}SiH_{0.72}$. These spectra generally exhibit a very broad band indicating a wide distribution of closely spaced hydrogen-bonding states (compared, e.g., with the phonon spectrum of crystalline CaH_2 also shown in the figure). This suggests that the hydrogen atoms reside in an unusual amorphous or nanocrystalline structure, consistent with the lack of a well-defined plateau in the isotherm plots. Such apparent spectral smearing is similar to that commonly observed in other amorphous hydride compounds such as $TiCuH_x$ [18] and $Pd_{85}Si_{15}H_x$ [19]. This interesting morphological behavior will be discussed in detail elsewhere in a separate publication. The formation of this amorphous structure is consistent with the observed disappearance of virtually all NPD reflections associated with the Ca_2Si phase upon hydriding [6].

Compared to Ca_2Si, the cation size in CaMgSi is contracted, so that the orthorhombic structure is less distorted ($a/c=0.90$ compared to $a/c=0.85$ in Ca_2Si). It should be noted that, in the C15 Laves phases [20], the atomic-size ratio is a decisive factor controlling the occurrence of hydrogen-induced amorphization. Similarly, the less strained CaMgSi with decreased

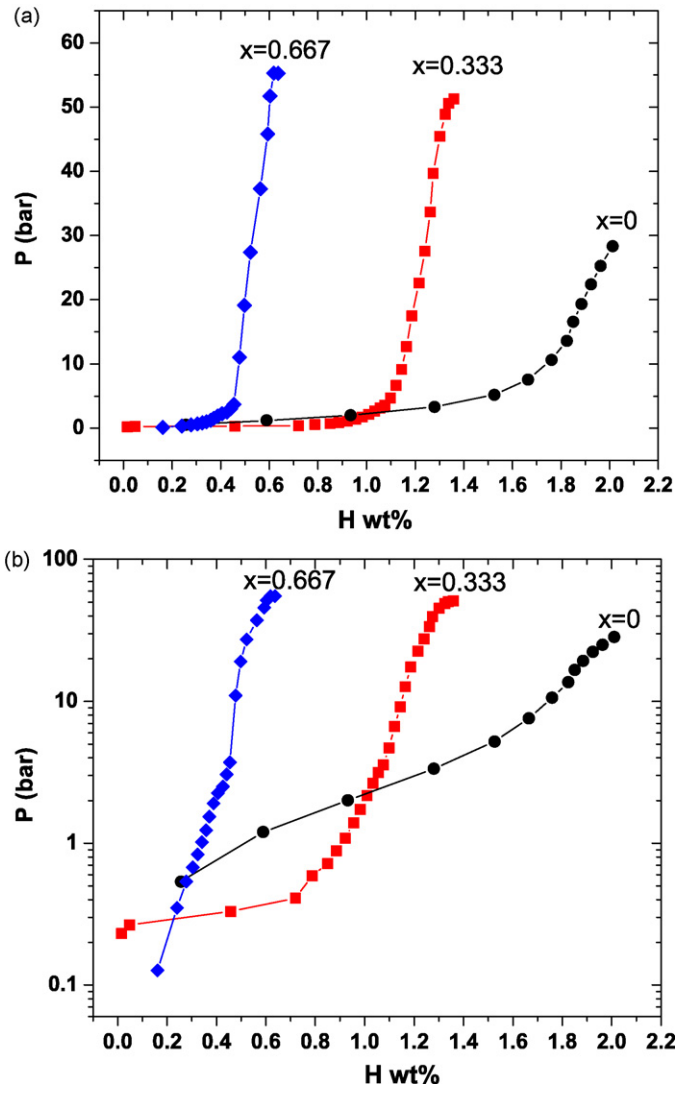

Fig. 4. (a) Absorption isotherms for $Ca_{2-x}Mg_xSi$ within the composition range $0 \le x \le 1$ at 473 K. CaMgSi ($x = 1$) does not noticeably absorb hydrogen up to 7 MPa H_2 and 473–573 K, and therefore is not plotted. (b) Logarithmically scaled isotherm plots indicating the general lack of an obvious pressure plateau.

$R_{Ca,Mg}/R_{Si}$ atomic-size ratio would be less easily amorphized by hydrogenation. In addition, the crystal structure indicates (see Fig. 3 inset) that all Mg atoms only occupy the unshared edges of the cation trigonal prismatic columns that run parallel to the *a* axis and also can be viewed as sheets of shared prisms normal to the *c* axis. The bonding between Si and cations (2 Mg and 1 Ca) also serves to adhere the cation trigonal prismatic sheets together. In Ca_2Si, Si is significantly off-centered in the trigonal prism with distances to the prismatic cations in the range of 2.74–3.30 Å, whereas they are within the range of 2.73–3.20 Å in CaMgSi. Consequently, the unique substitution of Mg can produce a less distorted, ordered structure with more symmetric bonding. (N.B.: it should be remembered that Mg_2Si with a cubic structure and highly symmetric bonding is very difficult to hydrogenate.) These two structural features may plausibly explain the difficulties in hydriding and forming amorphous hydrides from CaMgSi.

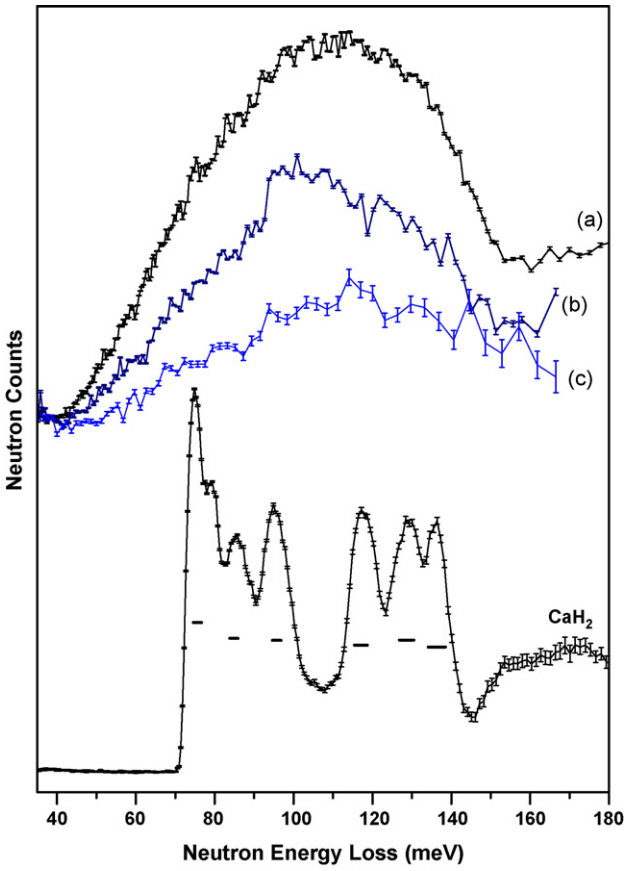

Fig. 5. Neutron vibrational spectra (at 5 K) for hydrides of: (a) Ca_2Si, (b) $Ca_{1.667}Mg_{0.333}Si$, and (c) $Ca_{1.333}Mg_{0.667}Si$ synthesized at 473 K and 7 MPa H_2, compared to that of CaH_2 (from Ref. [9]). Instrumental resolution (FWHM) is depicted by horizontal bars beneath the spectra.

4. Conclusions

Unlike the solid-solution phases formed in the analogous $Ca_{2-x}Mg_xSn$ system, $Ca_{2-x}Mg_xSi$ ($0 \le x \le 1$) ternary systems are found to form only $(1-x)Ca_2Si + xCaMgSi$ two-phase mixtures. Although, the Ca_2Si component in these mixtures displays intriguing hydrogen absorption properties such as rapid absorption rates and hydrogen-induced amorphization, the CaMgSi component undergoes no appreciable hydrogen absorption for conditions up to 7 MPa H_2 and 473–573 K. Hence, combining the readily hydrided Ca_2Si alloy with the hard-to-hydride Mg_2Si alloy fails to produce a ternary silicide with improved hydrogen absorption properties and/or increased hydrogen wt.%.

Acknowledgment

This work was partially supported by DOE through EERE Grant No. DE-AI-01-05EE11104.

References

[1] J.J. Vajo, F. Mertens, C.C. Ahn, R.C. Bowman Jr., B. Fultz, J. Phys. Chem. B 108 (2004) 13977–13983.

[2] R.C. Jr. Bowman, S.–J. Hwang, C.C. Ahn, J.J. Vajo, Mater. Res. Soc. Symp. Proc., vol. 837, Materials Research Society, Pittsburgh PA, 2005, pp. 361–366.
[3] M. Aoki, N. Ohba, T. Noritake, S. Towata, Appl. Phys. Lett. 85 (3) (2004) 387–388.
[4] N. Ohba, M. Aoki, T. Noritake, K. Miwa, S. Towata, Phys. Rev. B: Condens. Matter 72 (2005), 075104.
[5] H. Wu, W. Zhou, T.J. Udovic, J.J. Rush, T. Yildirim, Phys. Rev. B: Condens. Matter 74 (2006) 224101.
[6] H. Wu, W. Zhou, T.J. Udovic, J.J. Rush, Chem. Mater. 19 (2007) 329–334.
[7] W.H. Zachariasen, C.E. Holley Jr., J.F. Stamper Jr., Acta Cryst. 16 (1963) 352.
[8] A.F. Andresen, A.J. Maeland, D. Slotfeldt-Ellingsen, J. Solid State Chem. 20 (1977) 93–101.
[9] H. Wu, W. Zhou, T.J. Udovic, J.J. Rush, T. Yildirim, J. Alloys Compd. 436 (2007) 51–55.
[10] E.N. Nikitin, E.N. Tkalenko, V.K. Zaitsev, A.I. Zaslavskii, A.K. Kuznetsov, Izvestiya Akademii Nauk SSSR Neorg. Mater. 4 (1968) 1902–1906.
[11] P. Manfrinetti, M.L. Fornasini, A. Palenzona, Intermetallics 8 (2000) 223–228.
[12] B. Eisenmann, H. Schaefer, A. Weiss, Z. Anorg. Allg. Chem. 391 (1972) 241–254.
[13] Certain commercial suppliers are identified in this paper to foster understanding. Such identification does not imply recommendation or endorsement by the National Institute of Standards and Technology, nor does it imply that the materials or equipment identified are necessarily the best available for the purpose.
[14] J.K. Stalick, E. Prince, A. Santoro, I.G. Schroder, J.J. Rush, in: D.A. Neumann, T.P. Russell, B.J. Wuensch (Eds.), Neutron Scattering in Materials Science II, Mat. Res. Soc. Symp. Proc., vol. 376, Materials Research Society, Pittsburgh, PA, 1995, p. 101.
[15] A.C. Larson, R.B. Von Dreele, General Structure Analysis System, Report LAUR 86-748, Los Alamos National Laboratory, NM, 1994.
[16] T.J. Udovic, D.A. Neumann, J. Leão, C.M. Brown, Nucl. Instrum. Methods Phys. Res., Sect. A 517 (2004) 189.
[17] A.K. Ganguli, A.M. Guloy, J.D. Corbett, J. Solid State Chem. 152 (2000) 474–477.
[18] J.J. Rush, J.M. Rowe, A.J. Maeland, J. Phys. F 10 (1980) L283–L285.
[19] J.J. Rush, T.J. Udovic, R. Hempelmann, D. Richter, G. Driesen, J. Phys.: Condens. Matter 1 (1989) 1061–1070.
[20] K. Aoki, Mater. Sci. Eng., A 304–306 (2001) 45–53.